Environmental Science Nano

Biodegradable Nanoparticles Aid the Gut Microbial Community in Delaying Antibiotic Resistance Emergence

Journal:	*Environmental Science: Nano*
Manuscript ID	EN-ART-04-2024-000382.R1
Article Type:	Paper

Statement of significance

The emergence of antibiotic resistance poses an urgent global health threat, underscoring the need for alternative antimicrobial approaches with minimal ecological impacts. This work demonstrates the potential for biodegradable nanoparticles (NPs) loaded with antibiotics to combat enteropathogens while safeguarding commensal gut microbes and reducing the emergence of antibiotic-resistance genes (ARG). This unique study presents synthetic Poly-lactic-co-glycolic acid (PLGA) and a plant-based Lignin-grafted PLGA (LNP) biodegradable NPs combined with a commonly used gastrointestinal antibiotic in swine, Enrofloxacin, that efficiently inhibits microbial growth and are not cytotoxic to intestinal cells at significantly low concentrations. This study elucidates the impacts of antibiotic-loaded biodegradable nanoparticles on the composition, function, and antibiotic resistance of the pig anaerobic gut microbiota. The insights gained highlight promising applications for nano-enabled drug delivery to target pathogens while avoiding collateral damage to the gut microbiome.

ARTICLE

Biodegradable Nanoparticles Aid the Gut Microbial Community in Delaying Antibiotic Resistance Emergence

Genesis Herrera[1], Sachin Paudel[2], Simone Lupini[1], Carlos Astete[3], Cristina Sabliov[3], and Debora Rodrigues[2†]

Received 00th January 20xx,
Accepted 00th January 20xx

DOI: 10.1039/x0xx00000x

The antibiotic-nanoparticle combinatorial effects on gut microbiome diversity, abundance, and antibiotic resistance remain largely unknown. In the present study, we investigated the potential impacts of biodegradable nanocarriers after one biocompatible dose that could promote sustainable treatment against enteropathogens. Enrofloxacin (Enro), a common antibiotic used in livestock, was loaded into biodegradable synthetic poly(lactic-co-glycolic) acid (PLGA) and plant-based Lignin (LIGNIN) nanoparticles. Anaerobic bioreactors containing fresh slurry collected from pig intestines were used to simulate the anaerobic gut microenvironment. Bioreactors were inoculated with empty NPs with concentrations identical to loaded nanoparticles and free Enro**,** PLGA (Enro) (PE), and LIGNIN(Enro) (LE) that present antimicrobial activity and non-cytotoxicity to pig intestinal cells. Slurry aliquots from the bioreactors were collected for RNA extraction after 24, 48, and 72 hours of exposure to the drug and nanocarriers for microbial 16S rRNA metatranscriptomics and resistome analysis. Our results showed that PLGA and PE microbial communities were similar over all periods despite containing Enro. The impact of LIGNIN on the microbial community was minimal since it was similar to the control. However, loaded LE significantly reduced the microbial diversity but maintained essential estimated metabolic functions. Free Enrofloxacin affected the microbial community the most by decreasing the core gut microbiome diversity. Our results indicate that NP encapsulation of antibiotics delayed the increase in antibiotic resistance genes (ARG) expression between 24 and 72 hours compared to free Enro. These results demonstrate that the antibiotic treatment conveyed by NPs slows the rate of expression of ARG and reduces the adverse antibiotic effects on the gut microbial community.

Keywords: antibiotic-nanoparticle combinatorial treatment, nano drug delivery system (NDDS), antibiotic resistance genes (ARGs), antibiotic resistome

Introduction

The complex gut microbiome is vital for modulating host health, metabolism, immunity, and protection from pathogens.(1) Disruption of gut homeostasis, known as dysbiosis, compromises health through loss of beneficial microbes, overgrowth of pathogens, and reduced diversity.(1) Dysbiosis is linked to gastrointestinal, metabolic, immune, neurological, and other diseases.(1) Most microbiome research relies on fecal sampling, which does not fully represent distinct gastrointestinal tract regions. Pigs offer an advantageous model with nearly identical digestive system anatomy, physiology, and genetics (>98%) to humans.(2) Furthermore, samples can be easily collected directly inside their intestinal tract. Their core microbiota also closely resembles that of humans.(3) Like humans, pigs require a healthy commensal microbiome for proper immune function and disease resistance, which antibiotics can disrupt.(4) Although not used in humans, Enrofloxacin is one of the most used antibiotics in livestock industries to treat infections generated by *Escherichia coli*, *Salmonella,* and other enteropathogens.(5) Antibiotic consumption also drives antibiotic resistance,(6) a rising global threat as resistant microbes can spread to humans. Therefore, due to human microbiota and physiology similarities, pigs provide a valuable model for exploring microbiome-antibiotic interactions relevant to human health. (3)

Nano-drug delivery systems (NDDS) promise targeted, sustained antibiotic release while avoiding repeated dosing that promotes antibiotic resistance emergence.(7, 8) Diverse NDDS have also been demonstrated to have higher efficacy and minimal side effects in mammalian cells,(7-9) but certain NDDS made of metal nanoparticles (NPs) have led to dysbiosis. Slow-release biodegradable nanoparticles, on the other hand, have not been well studied, and their effects on the gut microbiota are still largely unknown.(10-12) In the present study, we hypothesized that the slow drug release from biodegradable polymer nanoparticles could shield the core microbiome from antibiotic effects by reducing antibiotic dysbiosis and the emergence of

[1]*Graduate Student, Dept. of Biology and Biochemistry, University of Houston, Houston, TX, 77004*
[2]*Graduate, Dept. of Civil and Environmental Engineering, University of Houston, Houston, TX, 77004*
[3]*Professor, Dept. of Biological & Agricultural Engineering, Louisiana State University, Baton Rouge, LA, 70803*
† Corresponding author: *Debora Rodrigues*
Electronic Supplementary Information (ESI) available: Tables, and Figures are included in the **Supplementary Information**. See DOI: 10.1039/x0xx00000x

antibiotic resistance genes (ARG) compared to naked antibiotics. We explored interactions of poly(lactic-co-glycolic acid) (PLGA) and Lignin-graft-PLGA nanoparticles with pig slurry collected from the small intestine to determine the effects of the nanoparticles in the microbiome and resistome using metatranscriptomics.(13) Furthermore, we defined the core microbial community as the group of consistently present microbes in both control and treatment samples. A detailed explanation can be found in the methods section.(14) We analyzed the pig microbiome antibiotic resistome by Oxford Nanopore Technology (ONT) sequencing of RNA-derived cDNA to capture expressed ARGs at 24 and 72 hours post-treatment. This approach provided insight into biodegradable nanoparticle effects on resistome induction versus traditional antibiotic delivery.

The PLGA, Lignin, and Lignin grafted copolymers have already been successfully used as delivery vehicles for drug and gene delivery, bioimaging, biosensor applications, and tissue engineering.(8, 15) However, their effect on gut microbes and antibiotic resistance has been overlooked and not studied in physiologically relevant conditions. For example, there are reports of empty and CpG oligodeoxynucleotide-loaded PLGA NP effects on chicken and mouse gut microbiomes.(16) However, these studies do not reflect the overall picture of the safety and efficiency of these NPs loaded with antibiotics, which could cause major changes in the gut microbial community and ARG expression.(17) For the full-scale utilization of these polymer-based nanocarriers in medicine and drug delivery, it is essential to elucidate NP nano-bio interactions and understand the gastrointestinal tract (GI tract) microbial community changes and ARGs emergence since the gut microbial community represents the overall health of humans and mammals. Thus, in this study, we used the pig intestinal community as a model system and Enrofloxacin as a model antibiotic, as we aimed to understand the effect of PLGA and Lignin, as NDDS, in the intestinal microbial community and ARGs expression.

Experimental

Materials and methods

Ethical Statement: The pig slurry was obtained from an antibiotic-free USDA-authorized provider in Texas, USA. A composite sample containing fresh small intestine slurry from five pigs was collected and combined to obtain enough slurry material to be used for all technical replicates in this study. For each condition tested, three technical replicates for the 16S rRNA microbial community and the resistome experiments were sequenced.

Gut microbiome collection and culture conditions

The intestinal slurry from the pigs was collected from freshly slaughtered pigs weighing around 85 kg and never exposed to any antibiotic from the JJ Packing facility in Brookshire, TX. The intestinal slurry was immediately cultured in a swine nutritive medium simulating the gut environment with minor modifications (Supplementary Information, Table S1).(18-20) The pig slurry was inoculated in a 500 ml anaerobic bottle with swine nutritive medium in a 50% (v/v) concentration. The slurry was incubated at 37 °C in an anaerobic chamber (Shel Lab BACTRON Anaerobic workstation) using anaerobic mixed gas (AMG), which contained 4.9% carbon dioxide, 5% hydrogen, and nitrogen as a balance gas to maintain an anaerobic environment similar to the gut.(21, 22) To ensure an anaerobic environment, before incubation in the anaerobic chamber, the slurry and nutritive medium were purged with nitrogen gas for 5 min to eliminate any residual oxygen. The slurry and swine nutritive medium (50% (v/v) mixture were incubated in an anaerobic chamber for six weeks to allow the bacterial community to reach a steady state before any experiments.(23, 24) This steady state was crucial for ensuring that any observed changes during experiments were due to the treatment only.(25) During this incubation period, the nutritive medium was changed by decanting the slurry every two days, and 50% of the supernatant was removed and completed with the same amount of nutritive medium to ensure the same final volume of the slurry-nutritive medium.(20, 26) To ensure the slurry was homogenous, the slurry and gut nutritive medium were swirled to mix. The process was done in the anaerobic chamber. After the community reached a steady state, the sample was split into technical replicates for the treatments. To assess microbial community composition, DNA 16S rRNA sequencing was performed after the stabilization period, capturing both active and inactive microbial populations. Although this method differs from the RNA sequencing used to analyze the control group post-treatment, both approaches revealed similar microbial families, providing a consistent basis for comparison across different time points (**Figure S1**).

After stabilizing the intestinal microbial community for 6 weeks in the nutritive media, six batch-type reactor systems were set up in triplicates to study the effect of the drug and drug-loaded NPs synthesized. The synthesis and characterization of the NPs are presented in our previous work.(8) Each triplicate batch bioreactor with the microbial communities was exposed to free Enrofloxacin (Enro) drug, empty PLGA nanoparticles (PLGA), Enrofloxacin loaded PLGA nanoparticles (PE), empty Lignin grafted PLGA nanoparticles (Lignin), and Enrofloxacin loaded in Lignin grafted PLGA nanoparticles (LE). The biocompatible concentrations for Enro, PE, and LE were 0.14, 0.18, and 0.20 μg/mL, respectively, which were determined in our previous work based on the minimum inhibitory concentration (MIC_{50}) against pathogenic *E.coli* O157:H7 and percent cell viability against the intestinal IPEC-J2 pig cell line.(8) The testing concentration for drug-free PLGA and Lignin nanoparticles was based on the equivalent weight of biocompatible PE and LE concentrations, respectively.(8) The stable bacterial community was treated with biocompatible concentrations of the respective drug, drug-loaded, and empty nanoparticles, and incubated at 37 °C in an anaerobic environment with a maximum retention time of 72 h. The media was not changed after the drug and drug-loaded nanoparticles were introduced to the slurry; the retention time of 72 h aimed to resemble the maximum gastrointestinal transit time of piglets and maximum drug release time for synthesized PE and LE nanoparticles.(8, 27) Aliquots of 15 mL samples were collected at 24, 48, and 72 h for RNA extraction and further downstream data processing.

Enrofloxacin Encapsulation with Lignin and PLGA Nanoparticles

Details about the synthesis and characterization can be found in our previous publications. (28, 29) The synthesis of PLGA and Lignin (Lignin-grafted-PLGA) NPs with and without antibiotics is briefly described below:

Enrofloxacin was encapsulated into PLGA nanoparticles (PLGA(ENRO) NPs) using a single emulsion evaporation technique based on the method outlined by Astete and Sabliov.(30) Initially, 440 mg of PLGA and 44 mg of Enrofloxacin were dissolved in 8 mL of ethyl acetate and 2.4 mL of acetone with mild stirring for 30 minutes at room temperature to form an organic phase. Simultaneously, 2000 mg of poly (vinyl alcohol) PVA was dissolved in 100 mL of nanopure water at 86 °C until fully dissolved. Then, 64 mL of this PVA solution was mixed with 6.4 mL of ethyl acetate to create an aqueous phase. The organic phase was added dropwise into the aqueous phase while subjecting it to probe sonication at 750 W for 15 min in pulse mode at 40% amplitude using an ice bath. Ethyl acetate was evaporated under vacuum for 40 min at 33 °C and 80 rpm using a rotavapor. Post-encapsulation, PLGA(ENRO) NPs were purified by centrifugation at 120,000 x g for 30 min, followed by resuspension in nanopure water, a second centrifugation at 120,000 x g for 2 h, and resuspension in ultrapure water. Trehalose was added in two steps: 950 mg after the first centrifugation and 450 mg after the second to stabilize the nanoparticles during freezing and drying. The sample was divided into eight vials, stored at -80 °C overnight, and then for the freeze-drying steps of nanoparticle preparation, we used a FreeZone 2.5 Liter -84°C Benchtop Freeze Dryer from Labconco Corporation (Kansas City, MO). The vacuum pressure during the freeze-drying process was maintained at approximately 0.131 mbar. Both temperature and pressure were monitored and regulated throughout the process to ensure consistent and effective lyophilization of the samples. Finally, the lyophilized PLGA(ENRO) NPs were stored in -20 °C until needed.(28, 30) For the lignin-grafted PLGA nanoparticles, lignin was grafted to PLGA using a method detailed by Astete and Sabliov.(30)

Subsequently, both empty and Enrofloxacin-loaded Lignin nanoparticles were prepared by dissolving 900 mg of Lignin-PLGA and 70 mg of Enrofloxacin (or no Enrofloxacin for empty nanoparticles) in 14 mL of ethyl acetate at room temperature with vigorous agitation. The organic phase was then combined with 150 mL of water (aqueous phase) and mixed for 15 min at room temperature, followed by high-pressure homogenization at 30,000 psi with four passes at 4 °C using Microfluidics Corp. equipment. Ethyl acetate was evaporated using a Buchi Corporation rotavapor R-300 at 33 °C under vacuum for 80 min. Cryoprotectant trehalose was added to the polymeric nanoparticle suspension at a ratio of 1:1 (w/w) and mixed for 20 min. The nanoparticle suspension was frozen at -80 °C before undergoing freeze-drying for 2 d at -80 °C using a FreeZone 2.5 system from Labconco Corporation. Both types of nanoparticles were stored at -20 °C.(29)

RNA Extraction and cDNA Transformation

After treating each fresh pig slurry in the anaerobic bioreactor, 15 mL of the slurry was collected at 24, 48, and 72 hours for RNA extractions. According to the manufacturer protocol, the RNA extractions were conducted with the Quick-RNA Fungal/Bacterial Miniprep (Zymo Research, Irvine, CA, USA). The sample was pretreated at -20 °C overnight and then extracted for RNA for higher quality control and quantity yield. Once removed, the RNA was immediately converted to cDNA with the kit SuperScript IV Reverse Transcriptase (Invitrogen, Life Technologies, Carlsbad, CA) according to the kit's protocol. An Agilent BioTek bioanalyzer and a Qubit Broad Range RNA and DNA assays were used to determine the purity and integrity of the extracted RNA. RNA converted to cDNA was immediately stored at -20 °C for further use.

Taxonomy Assignment and FASTQ Processing

The Mk1C device basecalled the sequences and processed the fastq files with q-scores above 7. The fastq files were used for the downstream analysis and submitted to the NCBI Genebank with the BioProject ID: PRJNA784703. The taxonomy for each Fastq file was assigned using the Usearch sintax command (usearch11 version) and the 16S database (RDP 16S training set v16, RTS).(31) After the classification, each sample generated (.SINTAX) files was pre-processed with seven R scripts from Mann and collaborators to filter information and create a count table.(32, 33) The R-scripts generated an operational taxonomical unit (OTU) table.(34) The OTU file and the created mapping file were imported into the MicrobiomeAnalyst web-based platform for metatranscriptomics and statistical analysis.(32, 33)

16S rRNA Metatranscriptomics Data and Statistical Analysis

The metatranscriptomics data was further filtered, normalized, and analyzed in the MicrobiomeAnalyst using the default parameters in the interface to remove low-quality reads.(33) The reads with low abundance in all samples were removed by using a low count filter set to 10% prevalence in the sample and minimum count = 2. The low variance filter was set to 10% to remove and based on the inter-quantile range. The normalization was done by data transformation of relative log expression. The community profiling was done using different statistical analyses.(33) The abundance profiling feature created the phylum and genus relative abundance charts.(32, 33) The α (alpha) diversity was determined based on the Shannon index.(35) The metatranscriptomics data was further filtered, normalized, and analyzed in the MicrobiomeAnalyst using the default parameters in the interface to remove low-quality reads.(33) The low abundance of reads in all samples was removed. The community profiling was done using different statistical analyses.(33) The abundance profiling feature created the phylum and genus relative abundance charts.(32, 33) The α (alpha) diversity was determined based on the Shannon index.(35) Additional information on statistical analysis and software used is included in the supplemental information.

Estimation of Metabolic Function via 16S rRNA

The FASTQ sequences generated from sequencing with the MinIon platform were imported into the R studio and processed using the DADA2 pipeline. The parameters, such as a maximum number of expected errors (maxEE), minimum length (minLen), and max number of Ns (MaxN) for the sequence filtering, were set as: minLen = 200, maxN=0, maxEE=10.

The sequences that passed the filter were used to determine the error rate, dereplication, and removal of chimeric sequences. The unique amplicon sequence variants (ASVs) obtained were then imported into Python and analyzed using the default parameters of the PICRUSt2 pipeline. The inferred metabolic functions were exported

as Kegg Orthology (KO) and mapped into the putative metabolic pathways (BRITE). Using the functions included in the R-Studio package vegan,(36) PROTEST,(37) and PROCSRUSTES,(38) a correlation between the inferred metabolic functions and the taxa was examined.

Resistome Analysis via Antibiotic Resistance Genes Identification

The fastq files from the Barcoding Kit 96 (SQK-RBK110.96) were obtained after the MinION Mk-1C basecalled the reads. The files were uploaded to the Oxford Nanopore Technologies EPI2ME desktop agent for the downstream analysis using the Fastq Antimicrobial Resistance v2021.05.17 workflow that uses the comprehensive antibiotic resistance database (CARD) via the resistance gene identifier that predicts resistome based on homology.(39, 40) The sequences were blasted against antibiotic-resistant genes in the database. The fastq files were used for the downstream analysis and submitted to the NCBI Genebank with the BioProject ID: PRJNA813149. RStudio and R programming software were used to normalize with ARG relative log and create NMDS, network analysis, alpha diversity, and heatmap.(41) Furthermore, the NMDS plot describing the relationship of ARGs across all samples, post 48 h samples were clustered together, indicating high similarity, and thus our ARG analysis focused on 24 and 72 hours (**Figure S5**). The RNA was chosen over the DNA to detect expressed functional ARG from the changing microbial community**.**

Results and discussion

Impact of Antibiotic-Loaded Nanoparticles on Microbial Composition

As expected, the taxonomic analysis of the pig slurry showed shared taxa with the human gut microbiome, which were composed of *Fusobacterium*, *Ruminococcus*, *Peptostreptococcus, Clostridium, Cloacibacillus, Roseburia, Escherichia, Blautia, Alistipes*, and *Desulfovibrio.*(42-45) Other taxa were also found in pigs, not necessarily in the human gut microbiome. However, this shared sub-population accounted for 95% of the pig microbiota and was defined as the "core." The top twenty most relatively abundant genera are presented in **Figure 1A** by sample and treatment conditions. Microbial community changes were investigated at three time points (24, 48, and 72 hours) for all treatment conditions and the control group. Relative to the alpha diversity (expressed as Shannon Index), the different treatments with drug and drug-loaded NPs shifted the population of certain microbes, leading to a visible change in alpha diversity compared to the controls (**Figure 1B-C**). In the free antibiotic treatment, in addition to the reduction of about 10% in the initial microbial diversity after 48 h through 72 h **(Figure 1B-C),** there was a substantial loss of certain genera, such as *Shigella*, *Roseburia*, *Clostridium XIVb*, and *Anaerosalibacter*. Apart from eliminating *E. shigella,* a bacterial genus that can potentially cause diarrhea,(46) the Enro treatment also drastically reduced the percent abundance of Firmicutes, such as *Roseburia* (from 13% to 1%) and *Clostridium XIVb* (from 5% to 0.1%). These gut environment commensals are responsible for maintaining gut homeostasis by producing short-chain fatty acids (SCFAs) like butyrate and mobilizing dietary components, such as carbohydrates, non-starch polysaccharides, and fibers, to simulate their growth.(47, 48) The sharp decrement in alpha diversity value related to the Enro treatment and loss of Firmicutes phylum indicate that the bactericidal effect of the free drug can target specific subpopulations of the community, suggesting that Proteobacteria and Firmicutes are highly susceptible to free Enro.(47, 48)

Furthermore, this result indicates that administering free Enro might increase the risk of several diseases by changing the microbial community's equilibrium and inducing dysbiosis. Ma and colleagues found a similar outcome with the loss of Proteobacteria and Firmicutes in a different animal model, i.e., neonatal chickens treated with Enrofloxacin antibiotics.(49) Overall, it was observed that the free drug exhibited rapid effects on the microbial community within 24 h, whereas the loaded antibiotics in NPs took longer (72 h) to show an impact. Similar results were observed in this study with PE and LE nanoparticles compared to the free drug. This delayed effect of loaded NPs can be attributed to the slow and continuous release of the drug from the NPs.(8, 28)

Furthermore, our study observed a minimal change in alpha diversity over time when the gut microbiome was treated with empty PLGA NPs.(50) On the other hand, empty Lignin alpha diversity was lower than the control and more like free Enrofloxacin. This difference between PLGA and Lignin empty NPs could be related to the binding affinity of Lignin to bile.(51) The lack of bile as a nutrient can affect the proliferation of microorganisms from the class Clostridia, which can metabolize primary bile with consequent production of secondary bile acids used by other gut microbes.(52)

Interestingly, the microbiome associated with empty PLGA NPs was like the control. Even though the core microbial community with the empty PLGA treatment did not change significantly, the microbial community composition was still altered by the presence of the nanoparticle. More specifically, *Peptostreptococcus* and *Desulfovibrio* increased with the PLGA treatment, whereas the abundance of *Roseburia* substantially decreased (from 14% to 1%). PLGA is a recognized biodegradable polymer that decomposes into lactic and glycolic acids. Lactic acid can be metabolized further to produce lactate. A study found that lipase, an enzyme that can be secreted by microbes or by other enzymes from the hydrolase family, plays a significant role in the enzymatic degradation of PLGA. This degradation occurs through the cleavage of ester bonds in aliphatic polyesters. However, the enzyme catalytic performance depends on the microbial source because the substrate binds to structural variations around the ester linkage.(53) The ability of PLGA to be metabolized by the gut microbiota likely contributed to the observed shifts in microbial populations. Previous studies have reported that increased lactic acid levels favor the growth of *Peptostreptococcus* and *Desulfovibrio* genera, as observed in our study with PLGA.(54, 55)

Even though the biodegradation of the PLGA NPs altered some microbial-specific genera, the alpha diversity index, with a p-value of 0.05 from a one-way ANOVA, like the control, showed no adverse effects on the core microbial population. Previous studies have demonstrated the capability of lipase secretion by F*usobacterium, Ruminococcus,* and

Peptostreptococcus, which were also present in this study.*(56)* These genera could have aided in PLGA biodegradation. In the case of PE NPs, the microbial diversity was characterized by a near-constant alpha-diversity score during the different time points and by a higher similarity to free Enro compared to PLGA (**Figure 1B**). A modest decrease in the alpha diversity was seen at 48 h, as was previously noted for free Enro, which could be associated with the previously mentioned genera-specific antibacterial action.

Interestingly, the alpha diversity value for PE at 72 h was recovered and was equivalent to empty PLGA and controls. This finding implies that PE therapy could lessen the long-term harmful effects of pure antibiotics on the microbial community by increasing microbial diversity. However, the LE treatment compared to empty Lignin and the controls at 48 and 72 h presented a significant drop in the alpha diversity index, p-value of 0.05 from a one-way ANOVA. This could be due to a combinatorial effect for the free antibiotic and the empty Lignin NP, which led to a shift in the microbial community. Among the genera that have benefited the most from this potential combinatorial effect is *Fusobacterium.* More specifically, the percent abundance of *Fusobacterium* increased by over 150% compared to the control. Despite being considered a commensal gut bacteria in humans and other animals, *Fusobacterium* has been typically associated with increased inflammation and development of colorectal cancers when in high abundance in the gut.(57)

Differential Effects of Lignin and PLGA Nanoparticles on Temporal Anaerobic Microbiome Changes with Antibiotic Treatments

The combinatorial effects of antibiotics and NPs on the gut microbiota were elucidated by examining the microbial community changes concerning treatment parameters, including the presence or absence of antibiotics, nanoparticle type, and length of exposure. Beta diversity analysis enabled the comparison of the microbiota between experimental groups. We applied a non-metric multidimensional scaling (NMDS) to the beta diversity data acquired from the bacterial genera associated with the various conditions (**Figure 1C**). The beta diversity analysis demonstrated apparent differences in how Lignin and PLGA nanoparticles impacted microbial communities depending on whether they were loaded with antibiotics.

For Lignin, there were drastic changes in microbiota composition between loaded and unloaded particles. In contrast, empty PLGA and Enrofloxacin-loaded PLGA (PE) NPs had similar beta diversity despite the presence of the drug. The results showed that PLGA NPs mitigated the adverse effects of free Enrofloxacin on the microbial community. Loading Lignin with Enro shifted community structure compared to empty particles, clustering more closely with the antibiotic-only treatment. This indicates that the drug, not the Lignin carrier, primarily drove the microbiome alterations with loaded Lignin NPs. **Figure 1C**, which represents the similarity between microbial communities among all experimental conditions, shows the time dependency effect of free drug and drug-loaded NPs in the microbial community with a p-value less than 0.02 from a PERMANOVA. According to the beta diversity with the NMDS analysis, the clustering was mainly brought on by the antibiotic-nanoparticle combinatorial effect. From this analysis, except for Enro at 24 h, we could distinguish, regardless of the time, a separate cluster associated with the presence of the antibiotic (**Figure 1C,** highlighted in the yellow ellipse). For empty NPs and controls, the separation was based on time, with a cluster for 24 h (highlighted in the green ellipse) and a combination of 48 and 72 h (highlighted in the purple ellipse). This was further corroborated by the clustered heatmap (**Figure S4**). The heatmap indicated that the treatments influenced the microbial diversity differently than the free drug. However, for drug-loaded PE and LE NPs, the microbial community responded less drastically to the pure antibiotic. Furthermore, the impact was less immediate than that of the free antibiotic, which was observed with a higher change at 48 h (**Figure S4**), as opposed to 72 h for PE and LE. Our previous drug release studies for Lignin and PLGA NPs have shown that after 24 h, about 80% of the drug was released from the NPs and continued to be released for an extended period, explaining the sustained effects on the microbial community exposed to NPs throughout 24 to 72 h, with a peak effect at 72 hours.(8)

PLGA NPs are commonly used and desirable for drug delivery to protect the gut microbiome, maintain homeostasis, and prevent dysbiosis.(58) However, Lignin nanoparticles have also demonstrated good stability and prolonged drug release under intestinal conditions.(59) Lignin's heterogeneous structure and variability from different extraction methods can impact its antimicrobial, stability, and antioxidant properties, which may influence the anaerobic microbiome.(15) Our observations do not preclude Lignin's potential as a drug delivery system.(60) Based on the experimental conditions, including a static environment enriching certain microbes and using biocompatible concentrations for intestinal cells, it was impossible to confirm dysbiosis from any treatment. Hence, this result suggests these nanoparticles could be valuable for drug delivery. Especially considering that these nanoparticles in 24 h to 72 h have also been shown capable of undergoing endocytosis in the gut mammalian cells.(8) The endocytosis of the nanoparticles and the slow-release effects of the antibiotic combined could reduce the antibiotic's effects on the gut microbial community compared to the free drug.

ARTICLE

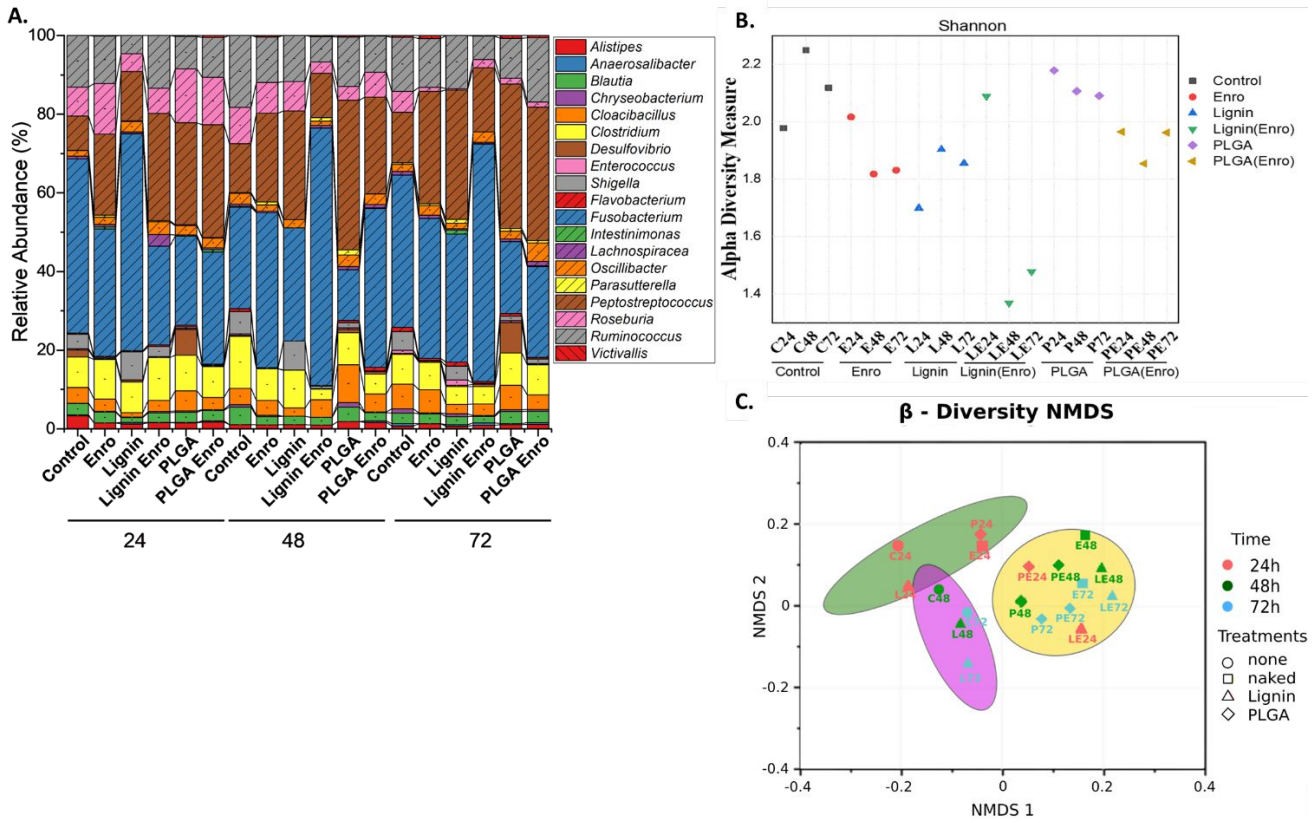

Figure 1. (A) Relative abundance of dominant gut microbial systems at the genus level. (B) Alpha diversity analysis chart using the Shannon Diversity Index. Box plot p-value: 0.05 from a one-way ANOVA F-value: 3.02. (C) Bray-Curtis's index beta diversity NMDS analysis for each treatment is based on the presence or absence of nanoparticles and antibiotics. Lignin indicates Lignin nanoparticles, PLGA indicates PLGA nanoparticles, naked indicates free Enro drug, and none indicates control. From a PERMANOVA F-value: 2.72; R^2: 0.37; p-value < 0.02. The notations 24, 48, and 72 indicate the microbial treatment conditions at the end of 24, 48, and 72 hours.

Impact of Antibiotic-Loaded Nanoparticles on Associated Metabolic Functions

Even though the various treatments produced detectable alterations in microbial composition, the high degree of overlap in metabolic pathways across small intestine anaerobic microbes suggests that relative abundance changes of specific taxa may not necessarily equate to important impairments of microbiome functionality.(61) To confirm that hypothesis, the potential changes in microbial community metabolic functions across different treatment conditions were estimated using the PICRUSt2 analysis of 16S rRNA sequences.(62) Alpha diversity of top-level pathways (KEGG: Kyoto Encyclopedia of Genes and Genomes) decreased at 24 h with free antibiotics compared to control. At the same time, nanoparticle treatments maintained metabolic diversity comparable to the control, likely due to the slow drug-release properties of the nanoparticles (**Figure S2A-B**). By 72 h, all Enrofloxacin treatments, except for PE, showed decreased alpha diversity (**Figure S2-B**). Secondary metabolic pathway shifts corroborated 16S community changes for PLGA NPs, with a higher diversity of metabolic functions, primarily related to lipid and glycan biosynthesis, compared to Lignin NPs and the control (**Figure 2A-B**). Lignin NPs and control exhibited similar metabolic functions. These results support earlier findings that the diversity of the microbial community is also impacted by the microbial community's capacity to consume byproducts or degrade biopolymers. Except for PLGA NPs, the overall results confirm the hypothesis that a reduction in the relative abundance of specific taxa does not automatically translate into a reduction in the microbial community metabolic potential. For instance, even though LE showed significant changes in the microbial alpha diversity compared to the control, the LE gut community could still potentially maintain the same metabolic activity as the control.

For both NPs loaded with Enro, the genetic information processing function was further examined to determine changes in homeostasis and housekeeping processes. PICRUSt2 prediction analysis indicated nanoparticle-antibiotic combinations and free Enro altered microbial composition. Yet, all these communities retained the genetic potential to maintain homeostasis and core metabolic processes, suggesting essential functional capacities were conserved despite taxonomic shifts. Therefore, biodegradable nanocarriers with antibiotics may allow for targeted antimicrobial effects while safeguarding the functional stability of the commensal gut microbiome.(43) Procrustes' statistical analysis,(38) visualized through NMDS ordination (**Figure 2C**), further substantiated the relationship between taxonomic (represented as squares) and predicted functional profiles (represented as circles). Metagenomic imputation of microbial metabolic potential clustered more tightly than phylogenetic ordination, with most functional matrices converging towards the center of the graph and the control. The wider dispersal of taxonomic matrices implied that community composition was more heavily impacted by nanoparticle and antibiotic treatments than metagenomically inferred functionality. These results suggest that we should consider the microbial community shifts, as many studies have done previously, and the overall community functionality to determine the impact of NPs and drugs in the gut microbiome.(16, 53, 63, 64) Overall, these results confirmed that the loaded nanoparticles do not generate dysbiosis.

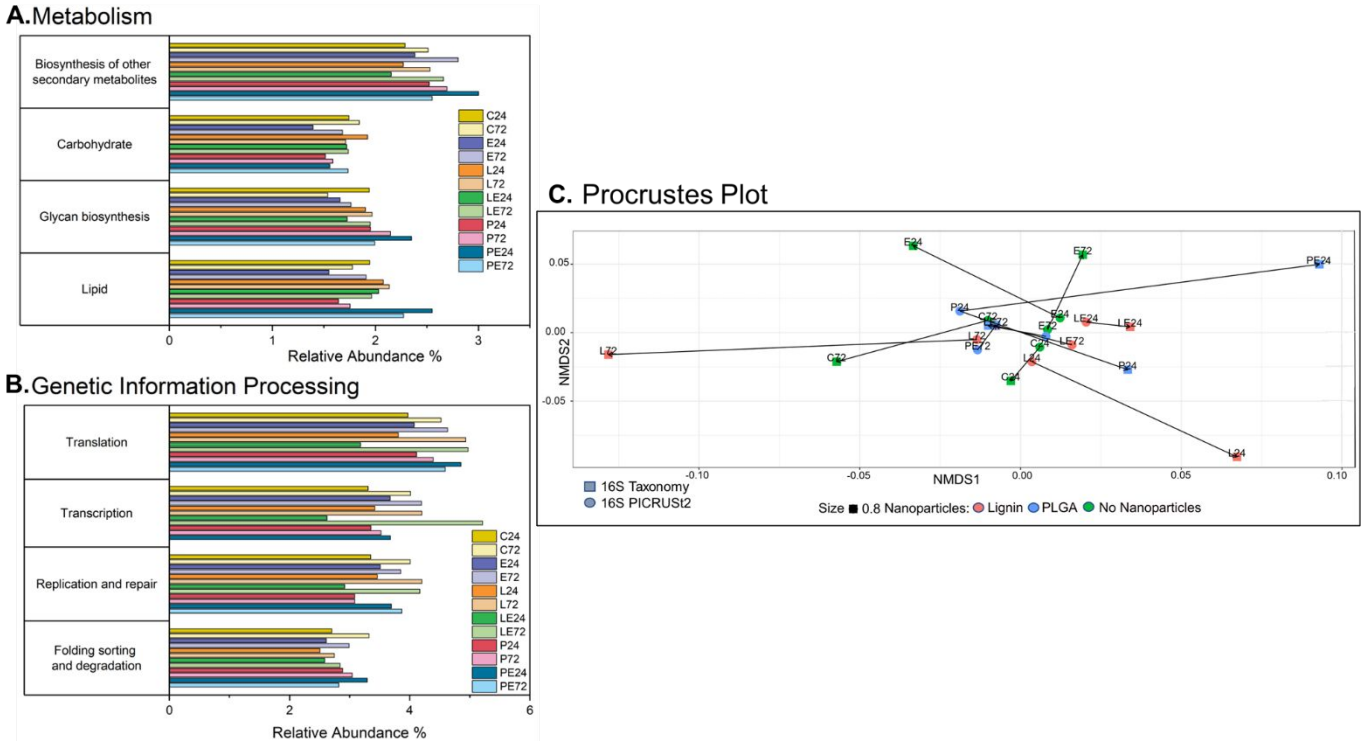

Figure 2. Estimated functional analysis with PICRUSt2 and comparison of estimated functions using Procrustes analysis. (A) KEGG BRITE Pathways show the metabolism and (B) Genetic Information, Processing functions level, estimated by PICRUSt2 using the 16S rRNA Fastq files for each condition during 24 and 72 hours post treatment indicating the decrease in functions occurring with the addition of Enrofloxacin but an increase with empty PLGA NPs. (C) Procrustes Plot comparing NMDS ordination of 16S microbial taxonomy and 16S PICRUSt2 functions. Correlation in a symmetric Procrustes rotation: 0.26 and Significance: 0.78.

Lignin and PLGA Minimize the Emergence of Antibiotic Resistant Genes Detected Within 72 Hours of the Initial Dose

Since the changes in the microbial community observed depended on nanoparticle type and the presence of Enrofloxacin, we investigated if these factors could also influence the microbial community resistome.(65) We hypothesized that disruptions to the intestinal microbiota would correspond with increased antibiotic resistance gene (ARG) expression. NMDS analysis (**Figures 1, 3, and S5)** revealed clusters of microbial community shifts. The results showed that the resistome alpha diversity between 24 and 72 h remained similar in the control and empty PLGA cases. For empty Lignin NPs and PE, the ARG alpha diversity increased over time. However, the opposite effect was observed with LE since a decrease was seen over time. The novelty of ARG's slow emergence in the case of LE was attributed to biocompatible concentrations, which corroborates literature findings that biodegradable polymers used for NDDS could potentially decrease or slow the emergence of ARGs when loaded with antimicrobial agents.(7) Our results, especially with LE, are promising since resistance to metal nanomaterial is a growing concern.(66) Most ARGs observed in this study involved 16S rRNA modifications conferring resistance through base substitutions/methylations at rRNA sites (**Figure S6A**).(67) Though not the canonical resistance mechanism for Enrofloxacin, rRNA methylations in pathogenic/antibiotic-producing bacteria provide moderate resistance or determine susceptibility, enhancing adaptation.(68) **Table S2** in the supporting information includes a general overview of the

antibiotic class mechanisms for the observed ARGs in this study. All conditions predominantly expressed genes associated with the binding of the 30S ribosomal subunit for protection against tetracycline antibiotics (*tet*32, *tet*O, *tet*Q, and *tet*W), enzymatic inactivation of lincomycin, aminoglycoside, and elfamycin antibiotics (*lnu*C, *ANT(6)-lb* and *EF-Tu*), methylation catalysis of rRNA for ribosomal alteration (*ErmG*), and point mutations in the 30S subunit of the 16S ribosomal RNA (*16S rRNA*, *rrs*D, *rrs*B, *rrs*H, *rrs*A, *rrn*B, and *rrs*C), which are common aminoglycoside antibiotic resistance mechanisms.(17, 39) The enzyme inactivation protein genes and the general schematic are shown in **Figure S6C**.(39) Though fluoroquinolone ARGs were expected in Enrofloxacin treatments, none were detected, possibly due to the low concentrations used (0.14-0.20 µg/mL) compared to ≥1 µg/mL typically used in free antibiotics.(69, 70) Despite this observation, Enrofloxacin increased aminoglycoside/tetracycline ARGs at 24 h, which subsided by 72 h, consistent with previous observations that Enrofloxacin can increase other ARG types.(69) Since Proteobacteria commonly hosts fluoroquinolone resistance genes but was considerably reduced with Enrofloxacin (**Figure S3**), this may explain the lack of detected fluoroquinolone ARGs.

Moreover, as expected, the increase in ARGs detected occurred in loaded NPs after 72 h, with minimal ARGs observed at 24 h, as shown by the heatmap and alpha diversity analysis in **Figure 3** using the CARD database. Interestingly, the expression of efflux pump ARGs such as *tet40*, *tetL*, *emrK*, *acrF*, and *mdtC* was mainly detected post 72 h in conditions containing Enrofloxacin, which is also a documented mechanism of resistance towards Enrofloxacin via extrusion of the drug by the efflux pumps.(39, 71) Efflux pumps are multicomponent molecular machines that span bacteria's inner cell and outer membrane to export several antibiotics.(71) The general schematic is shown in **Figure S6B**. The emergence of most efflux pump ARGs after a longer exposure time could be a sign of a potential capacity to delay the production of ARGs by the bacteria that the process of NPs encapsulation might have induced. The specific efflux pump ARGs that appear after 24 and 72 h are also evident in the Venn diagram for each NP loaded and empty, as compared with controls (free Enrofloxacin, no treatment) shown in **Figure S7**. A network analysis provided insight into bacteria expressing ARGs (**Figure S8)**. Free Enrofloxacin had the most connections with pathogenic bacteria and ARG diversity at 24 and 72 h. Most network vertices were associated with free Enrofloxacin, with fewer empty and loaded NPs, emphasizing NPs' benefits. No significant difference was observed in the resistome between NP types loaded with antibiotics (**Figure 3, S7**). However, loaded NPs showed reduced ARG diversity compared to free antibiotics or empty NPs.

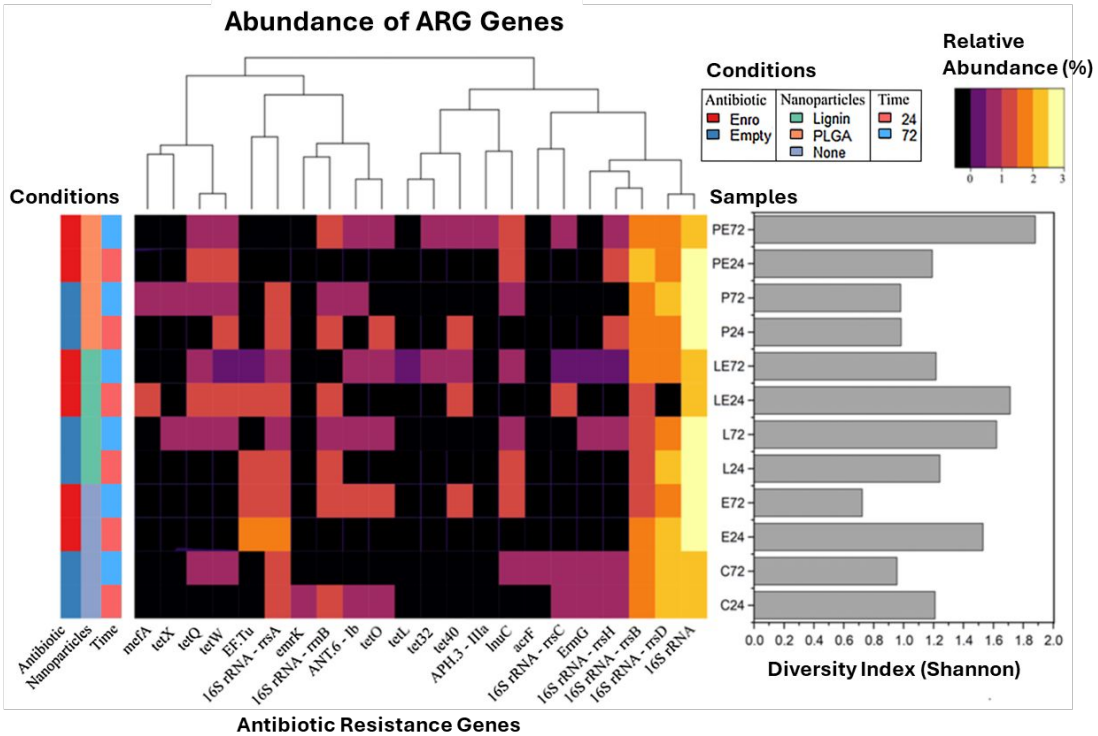

Figure 3. Antibiotic resistance genes clustered heatmap showing ARGs' hierarchal clustering and relative abundance in each condition. As part of the experimental factors, the clustered heatmap was created using Euclidean distance measures, including time, nanoparticle type, and antibiotic presence. The alpha diversity bar graph presents the Shannon Index and shows the ARG richness and abundance after each treatment for 24 and 72 hours; p-value: 0.58874; Mann-Whitney statistic:14.

Conclusions

This study demonstrates that free antibiotics notably disrupt the gut microbiome, decreasing diversity and rapidly inducing antibiotic resistance genes (ARGs). In contrast, empty Lignin nanoparticles minimize effects on the microbiome and resistome, exhibiting inherent biocompatibility. Loaded Lignin NPs restricted ARG induction compared to free drugs and outperformed loaded PLGA NPs in limiting ARG diversity

emergence, highlighting Lignin's promise as an antibiotic carrier. PLGA NPs maintained microbial diversity and hindered ARG enrichment when loaded, corroborating their established use as nanocarriers. Despite any changes in the microbial community's relative abundance, the estimated functional analysis showed that conservation in functions from the ending bacterial population could maintain metabolic functions and homeostasis. Lignin's unique properties could provide advantages over polymers like PLGA.(72) Optimizing Lignin NPs for controlled drug loading and release kinetics could enable a multifunctional platform for microbiome-targeted delivery. Biodegradable NPs enhanced antibacterial effects while protecting the microbiome and resistome at biocompatible concentrations. The Lignin NPs used in this study were synthesized using lignosulfonate alkali hydrolyzed to alkali Lignin NPs. The derivatization of the functional groups, such as hydroxyl (-OH) and carboxyl (-COOH), reduced the antimicrobial properties compared to pure Lignin NPs from other sources.(72) Furthermore, during the synthesis of the NPs, the alkali Lignin NPs were also conjugated with PLGA, further reducing the exposure of the phenolic groups and decreasing the antimicrobial activity.(73) This conjugation could also reduce PLGA core biodegradability, as the microbiota shift is not comparable to PLGA NPs.(72) This work indicates that optimized NP carriers could enable microbiome-sparing antibiotic delivery. However, to determine the applicability of NPs for antibiotic treatment, further studies on different NPs' drug release kinetics and polymer degradation byproducts in the GI tract are needed to fully elucidate differences in their effects on the microbial community and metabolomics. However, we acknowledge certain limitations in our study. The depth of our sequencing data is below typical standards. Still, our careful analysis and validation steps, combined with the advantages of longer read lengths, allowed us to draw meaningful conclusions. While our study utilized a single composite biological sample from five pigs with three technical replicates per condition, it is important to note that this approach may limit the generalizability of our findings.

Author Contributions

Genesis Herrera: Investigation, Methodology, Formal Analysis, Research Conceptualization, Data Curation, Validation, Visualization, Writing original draft - review & editing draft. **Sachin Paudel:** Investigation, Methodology, Data Curation, Research Conceptualization, Writing original draft. **Simone Lupini:** Data Curation, Validation, Visualization & Editing draft. **Carlos Astete**: Synthesis of nanomaterials and characterization. **Cristina Sabliov:** Research conceptualization, Project administration, synthesis of the nanomaterials, and characterization. **Debora F. Rodrigues:** Research Conceptualization, Methodology, Data Curation, Validation, Resource, Supervision, Visualization, Project Administration, Writing - review & editing, Funding Acquisition.

Conflicts of interest

The authors declare that the research was conducted without commercial or financial relationships construed as a potential conflict of interest. There are no conflicts to declare.

Acknowledgments

This work was supported by the Robert A. Welch Foundation, USA award number (E-2011-20190330), the NSF BEINM Grant Number:1705511, and by the United States Department of Agriculture (USDA), USA. National Institute of Food and Agriculture, AFRI project 2017-07878.

References

1. Fan Y, Pedersen O. Gut microbiota in human metabolic health and disease. Nature Reviews Microbiology. 2021;19(1):55-71.
2. Xiao L, Estellé J, Kiilerich P, Ramayo-Caldas Y, Xia Z, Feng Q, et al. A reference gene catalogue of the pig gut microbiome. Nature Microbiology. 2016;1(12):16161.
3. Gonzalez LM, Moeser AJ, Blikslager AT. Porcine models of digestive disease: the future of large animal translational research. Translational Research. 2015;166(1):12-27.
4. Ramirez J, Guarner F, Bustos Fernandez L, Maruy A, Sdepanian VL, Cohen H. Antibiotics as Major Disruptors of Gut Microbiota. Frontiers in Cellular and Infection Microbiology. 2020;10:731.
5. Foditsch C, Pereira RVV, Siler JD, Altier C, Warnick LD. Effects of treatment with enrofloxacin or tulathromycin on fecal microbiota composition and genetic function of dairy calves. PLOS ONE. 2019;14(12):e0219635.
6. Mahmood AR, Al-Haideri HH, Hassan FM. Detection of antibiotics in drinking water treatment plants in Baghdad City, Iraq. Advances in Public Health. 2019;2019:7851354.
7. Herrera G, Peña-Bahamonde J, Paudel S, Rodrigues DF. The role of nanomaterials and antibiotics in microbial resistance and environmental impact: an overview. Current Opinion in Chemical Engineering. 2021;33(100707):1-10.
8. Paudel S, Peña-Bahamonde J, Shakiba S, Astete CE, Louie SM, Sabliov CM, et al. Prevention of infection caused by enteropathogenic E. coli O157:H7 in intestinal cells using enrofloxacin entrapped in polymer based nanocarriers. Journal of Hazardous Materials. 2021;414:125454-63.
9. Mitchell MJ, Billingsley MM, Haley RM, Wechsler ME, Peppas NA, Langer R. Engineering precision nanoparticles for drug delivery. Nature Reviews Drug Discovery. 2021;20(2):101-24.
10. Lamas B, Martins Breyner N, Houdeau E. Impacts of foodborne inorganic nanoparticles on the gut microbiota-immune axis: potential consequences for host health. Particle and Fibre Toxicology. 2020;17(1):19.
11. Li Y, Yan N, Wong TY, Wang W-X, Liu H. Interaction of antibacterial silver nanoparticles and microbiota-dependent holobionts revealed by metatranscriptomic analysis. Environmental Science: Nano. 2019;6(11):3242-55.
12. Gangadoo S, Bauer BW, Bajagai YS, Van TTH, Moore RJ, Stanley D. In vitro growth of gut microbiota with selenium nanoparticles. Animal Nutrition. 2019;5(4):424-31.
13. Aguiar-Pulido V, Huang W, Suarez-Ulloa V, Cickovski T, Mathee K, Narasimhan G. Metagenomics, Metatranscriptomics, and Metabolomics Approaches for Microbiome Analysis. Evol Bioinform Online. 2016;12(Suppl 1):5-16.
14. Kokou F, Sasson G, Friedman J, Eyal S, Ovadia O, Harpaz S, et al. Core gut microbial communities are maintained by beneficial interactions and strain variability in fish. Nature Microbiology. 2019;4(12):2456-65.
15. Rico-García D, Ruiz-Rubio L, Pérez-Alvarez L, Hernández-Olmos SL, Guerrero-Ramírez GL, Vilas-Vilela JL. Lignin-Based Hydrogels: Synthesis and Applications. Polymers. 2020;12(1).
16. Chaplin A, Gao H, Asase C, Rengasamy P, Park B, Skander D, et al. Systemically-delivered biodegradable PLGA alters gut microbiota and

induces transcriptomic reprogramming in the liver in an obesity mouse model. Scientific Reports. 2020;10(1):13786.
17. Anand U, Carpena M, Kowalska-Góralska M, Garcia-Perez P, Sunita K, Bontempi E, et al. Safer plant-based nanoparticles for combating antibiotic resistance in bacteria: A comprehensive review on its potential applications, recent advances, and future perspective. Science of The Total Environment. 2022;821:153472.
18. Tanner SA, Zihler Berner A, Rigozzi E, Grattepanche F, Chassard C, Lacroix C. In Vitro Continuous Fermentation Model (PolyFermS) of the Swine Proximal Colon for Simultaneous Testing on the Same Gut Microbiota. PLOS ONE. 2014;9(4):e94123.
19. Macfarlane GT, Macfarlane S, Gibson GR. Validation of a three-stage compound continuous culture system for investigating the effect of retention time on the ecology and metabolism of bacteria in the human colon. Microbial Ecology. 1998;35(2):180-7.
20. Marcus Ian M, Wilder Hailey A, Quazi Shanin J, Walker Sharon L. Linking microbial community structure to function in representative simulated systems. Appl Environ Microbiol. 2013;79(8):2552-9.
21. Jost T, Lacroix C, Braegger CP, Chassard C. New Insights in Gut Microbiota Establishment in Healthy Breast Fed Neonates. PLOS ONE. 2012;7(8):e44595.
22. Tomas-Barberan F, García-Villalba R, Quartieri A, Raimondi S, Amaretti A, Leonardi A, et al. In vitro transformation of chlorogenic acid by human gut microbiota. Molecular Nutrition & Food Research. 2014;58(5):1122-31.
23. Aguirre M, Jonkers DMAE, Troost FJ, Roeselers G, Venema K. In Vitro Characterization of the Impact of Different Substrates on Metabolite Production, Energy Extraction and Composition of Gut Microbiota from Lean and Obese Subjects. PLOS ONE. 2014;9(11):e113864.
24. McDonald JAK, Fuentes S, Schroeter K, Heikamp-deJong I, Khursigara CM, de Vos WM, et al. Simulating distal gut mucosal and luminal communities using packed-column biofilm reactors and an in vitro chemostat model. Journal of Microbiological Methods. 2015;108:36-44.
25. Zegeye EK, Brislawn CJ, Farris Y, Fansler SJ, Hofmockel KS, Jansson JK, et al. Selection, Succession, and Stabilization of Soil Microbial Consortia. mSystems. 2019;4(4):10.1128/msystems.00055-19.
26. Chang Y, Hou F, Pan Z, Huang Z, Han N, Bin L, et al. Optimization of Culturomics Strategy in Human Fecal Samples. Frontiers in Microbiology. 2019;10:2891.
27. Snoeck V, Huyghebaert N, Cox E, Vermeire A, Saunders J, Remon JP, et al. Gastrointestinal transit time of nondisintegrating radio-opaque pellets in suckling and recently weaned piglets. Journal of Controlled Release. 2004;94(1):143-53.
28. Paudel S, Cerbu C, Astete CE, Louie SM, Sabliov C, Rodrigues DF. Enrofloxacin-impregnated PLGA nanocarriers for efficient therapeutics and diminished generation of reactive oxygen species. ACS Applied Nano Materials. 2019;2(8):5035-43.
29. Paudel S. Polymer-based nanocarriers to treat intestinal infection and reduce impact on gut microbiome: University of Houston; 2021.
30. Astete CE, Sabliov CM. Synthesis and characterization of PLGA nanoparticles. Journal of Biomaterials Science, Polymer Edition. 2006;17(3):247-89.
31. Edgar R. USEARCH v11 manual [Available from: https://drive5.com/usearch/manual/whatsnewv11.html.
32. Mann BC, Bezuidenhout JJ, Swanevelder ZH, Grobler AF. MinION 16S datasets of a commercially available microbial community enables the evaluation of DNA extractions and data analyses. Data in Brief. 2021;36:107036.
33. Shetty SA, Lahti L. Microbiome data science. Journal of Biosciences. 2019;44(5):115.
34. Team R. RStudio: Integrated Development for R. . 2021.09.1-372 ed. Boston, MA: PBC; 2020.
35. Shannon CE. A Mathematical Theory of Communication. Bell System Technical Journal. 1948;27(3):379-423.
36. Oksanen JAI. Vegan: an introduction to ordination. cran.r-project.org; 2015. p. 1-12.
37. Lisboa FJ, Peres-Neto PR, Chaer GM, Jesus Eda C, Mitchell RJ, Chapman SJ, et al. Much beyond Mantel: bringing Procrustes association metric to the plant and soil ecologist's toolbox. PLoS ONE. 2014;9(6):e101238-e46.
38. Goodall CR. Procrustes methods in the statistical analysis of shape. Journal of the Royal Statistical Society Series B-Methodological. 1991;53:285-321.
39. Alcock BP, Raphenya AR, Lau TTY, Tsang KK, Bouchard M, Edalatmand A, et al. CARD 2020: antibiotic resistome surveillance with the comprehensive antibiotic resistance database. Nucleic Acids Res. 2020;48(D1):D517-d25.
40. Coordinators NR. Database resources of the National Center for Biotechnology Information. Nucleic Acids Research. 2016;44(D1):D7-D19.
41. Conway JR, Lex A, Gehlenborg N. UpSetR: an R package for the visualization of intersecting sets and their properties. Bioinformatics. 2017;33(18):2938-40.
42. Bergamaschi M, Tiezzi F, Howard J, Huang YJ, Gray KA, Schillebeeckx C, et al. Gut microbiome composition differences among breeds impact feed efficiency in swine. Microbiome. 2020;8(1):110.
43. Gresse R, Chaucheyras Durand F, Dunière L, Blanquet-Diot S, Forano E. Microbiota Composition and Functional Profiling Throughout the Gastrointestinal Tract of Commercial Weaning Piglets. Microorganisms. 2019;7(9):343.
44. Yang G, Shi C, Zhang S, Liu Y, Li Z, Gao F, et al. Characterization of the bacterial microbiota composition and evolution at different intestinal tract in wild pigs (Sus scrofa ussuricus). PeerJ. 2020;8:e9124-e.
45. Rinninella E, Raoul P, Cintoni M, Franceschi F, Miggiano GAD, Gasbarrini A, et al. What is the Healthy Gut Microbiota Composition? A Changing Ecosystem across Age, Environment, Diet, and Diseases. Microorganisms. 2019;7(1):14.
46. Jafari F, Hamidian M, Rezadehbashi M, Doyle M, Salmanzadeh-ahrabi S, Derakhshan F, et al. Prevalence and Antimicrobial Resistance of Diarrheagenic Escherichia coli and Shigella Species Associated with Acute Diarrhea in Tehran, Iran. Canadian Journal of Infectious Diseases and Medical Microbiology. 2009;20:341275.
47. Guo P, Zhang K, Ma X, He P. Clostridium species as probiotics: potentials and challenges. Journal of Animal Science and Biotechnology. 2020;11(1):24.
48. Tamanai-Shacoori Z, Smida I, Bousarghin L, Loreal O, Meuric V, Fong SB, et al. Roseburia spp.: a marker of health? Future Microbiology. 2017;12(1746-0921 (Electronic)).
49. Ma B, Mei X, Lei C, Li C, Gao Y, Kong L, et al. Enrofloxacin Shifts Intestinal Microbiota and Metabolic Profiling and Hinders Recovery from Salmonella enterica subsp. enterica Serovar Typhimurium Infection in Neonatal Chickens. mSphere. 2020;5(5):e00725-20.
50. Whittaker RH. Evolution and measurement of species diversity. TAXON. 1972;21(2-3):213-51.
51. Rodríguez-Gutiérrez G, Rubio-Senent F, Lama-Muñoz A, García A, Fernández-Bolaños J. Properties of lignin, cellulose, and hemicelluloses isolated from olive cake and olive stones: binding of water, oil, bile acids, and glucose. Journal of Agricultural and Food Chemistry. 2014;62(36):8973-81.

52. Staley C, Weingarden AR, Khoruts A, Sadowsky MJ. Interaction of gut microbiota with bile acid metabolism and its influence on disease states. Appl Microbiol Biotechnol. 2017;101(1):47-64.
53. Kemme M, Prokesch I, Heinzel-Wieland R. Comparative study on the enzymatic degradation of poly(lactic-co-glycolic acid) by hydrolytic enzymes based on the colorimetric quantification of glycolic acid. Polymer Testing. 2011;30(7):743-8.
54. Huber Tl Fau - Cooley JH, Cooley Jh Fau - Goetsch DD, Goetsch Dd Fau - Das NK, Das NK. Lactic acid-utilizing bacteria in ruminal fluid of a steer adapted from hay feeding to a high-grain ration. American journal of veterinary research. 1976(0002-9645 (Print)).
55. Keller KL, Wall JD. Genetics and molecular biology of the electron flow for sulfate respiration in desulfovibrio. Frontiers in Microbiology. 2011;2:135-.
56. Alalawy AI, Guo Z, Almutairi FM, El Rabey HA, Al-Duais MA, Mohammed GM, et al. Explication of structural variations in the bacterial and archaeal community of anaerobic digestion sludges: An insight through metagenomics. Journal of Environmental Chemical Engineering. 2021;9(5):105910.
57. Wu J, Li Q, Fu X. Fusobacterium nucleatum Contributes to the Carcinogenesis of Colorectal Cancer by Inducing Inflammation and Suppressing Host Immunity. Translational Oncology. 2019;12(6):846-51.
58. Feng Z, Peng S, Wu Z, Jiao L, Xu S, Wu Y, et al. Ramulus mori polysaccharide-loaded PLGA nanoparticles and their anti-inflammatory effects in vivo. International Journal of Biological Macromolecules. 2021;182:2024-36.
59. Alqahtani MS, Alqahtani A, Al-Thabit A, Roni M, Syed R. Novel lignin nanoparticles for oral drug delivery. Journal of Materials Chemistry B. 2019;7(28):4461-73.
60. Niemi P, Aura A-M, Maukonen J, Smeds AI, Mattila I, Niemelä K, et al. Interactions of a Lignin-Rich Fraction from Brewer's Spent Grain with Gut Microbiota in Vitro. Journal of Agricultural and Food Chemistry. 2013;61(27):6754-62.
61. Thursby E, Juge N. Introduction to the human gut microbiota. Biochemical Journal. 2017;474(11):1823-36.
62. Ijoma GN, Nkuna R, Mutungwazi A, Rashama C, Matambo TS. Applying PICRUSt and 16S rRNA functional characterisation to predicting co-digestion strategies of various animal manures for biogas production. Scientific Reports. 2021;11(1):19913.
63. Panyam J, Labhasetwar V. Biodegradable nanoparticles for drug and gene delivery to cells and tissue. Advanced Drug Delivery Reviews. 2003;55(3):329-47.
64. Wan F, Bohr SSR, Kłodzińska SN, Jumaa H, Huang Z, Nylander T, et al. Ultrasmall TPGS–PLGA hybrid nanoparticles for site-specific delivery of antibiotics into Pseudomonas aeruginosa biofilms in lungs. ACS Applied Materials & Interfaces. 2020;12(1):380-9.
65. Kanger K, Guilford NGH, Lee H, Nesbø CL, Truu J, Edwards EA. Antibiotic resistome and microbial community structure during anaerobic co-digestion of food waste, paper and cardboard. FEMS Microbiology Ecology. 2020;96(2).
66. Nino-Martinez N, Salas Orozco MF, Martinez-Castanon GA, Torres Mendez F, Ruiz F. Molecular mechanisms of bacterial resistance to metal and metal oxide nanoparticles. International Journal of Molecular Sciences. 2019;20(11):1-15.
67. Doi Y, Arakawa Y. 16S ribosomal RNA methylation: emerging resistance mechanism against aminoglycosides. Clinical Infectious Diseases. 2007;45(1):88-94.
68. Salaikumaran MR, Badiger VP, Burra VLSP. 16S rRNA methyltransferases as novel drug targets against tuberculosis. The Protein Journal. 2022;41(1):97-130.
69. Li D, Gao J, Dai H, Wang Z, Duan W. Long-term responses of antibiotic resistance genes under high concentration of enrofloxacin, sulfadiazine and triclosan in aerobic granular sludge system. Bioresource Technology. 2020;312:123567.
70. Liu C, Yan H, Sun Y, Chen B. Contribution of enrofloxacin and Cu2+ to the antibiotic resistance of bacterial community in a river biofilm. Environmental Pollution. 2021;291:118156.
71. Piras C, Soggiu A, Greco V, Martino PA, Del Chierico F, Putignani L, et al. Mechanisms of antibiotic resistance to enrofloxacin in uropathogenic Escherichia coli in dog. Journal of Proteomics. 2015;127:365-76.
72. Astete CE, De Mel JU, Gupta S, Noh Y, Bleuel M, Schneider GJ, et al. Lignin-Graft-Poly(lactic-co-glycolic) Acid Biopolymers for Polymeric Nanoparticle Synthesis. ACS Omega. 2020.
73. Lee E, Song Y, Lee S. Crosslinking of lignin/poly(vinyl alcohol) nanocomposite fiber webs and their antimicrobial and ultraviolet-protective properties. Textile Research Journal. 2017;89(1):3-12.

Data availability statements

- The authors declare that the data supporting the findings of this study are available within the paper and its supplementary Information files. Should any data files be needed in another format they are available from the corresponding author upon reasonable request.
- All sequencing data have been deposited in the NCBI GenBank database under BioProject ID: PRJNA784703 and BioProject ID: PRJNA813149.”